Universidad Zaragoza

Instituto Universitario de Investigación en Nanociencia de Aragón
Universidad Zaragoza

Master Degree in Nanostructured Materials for Nanotechnology Applications

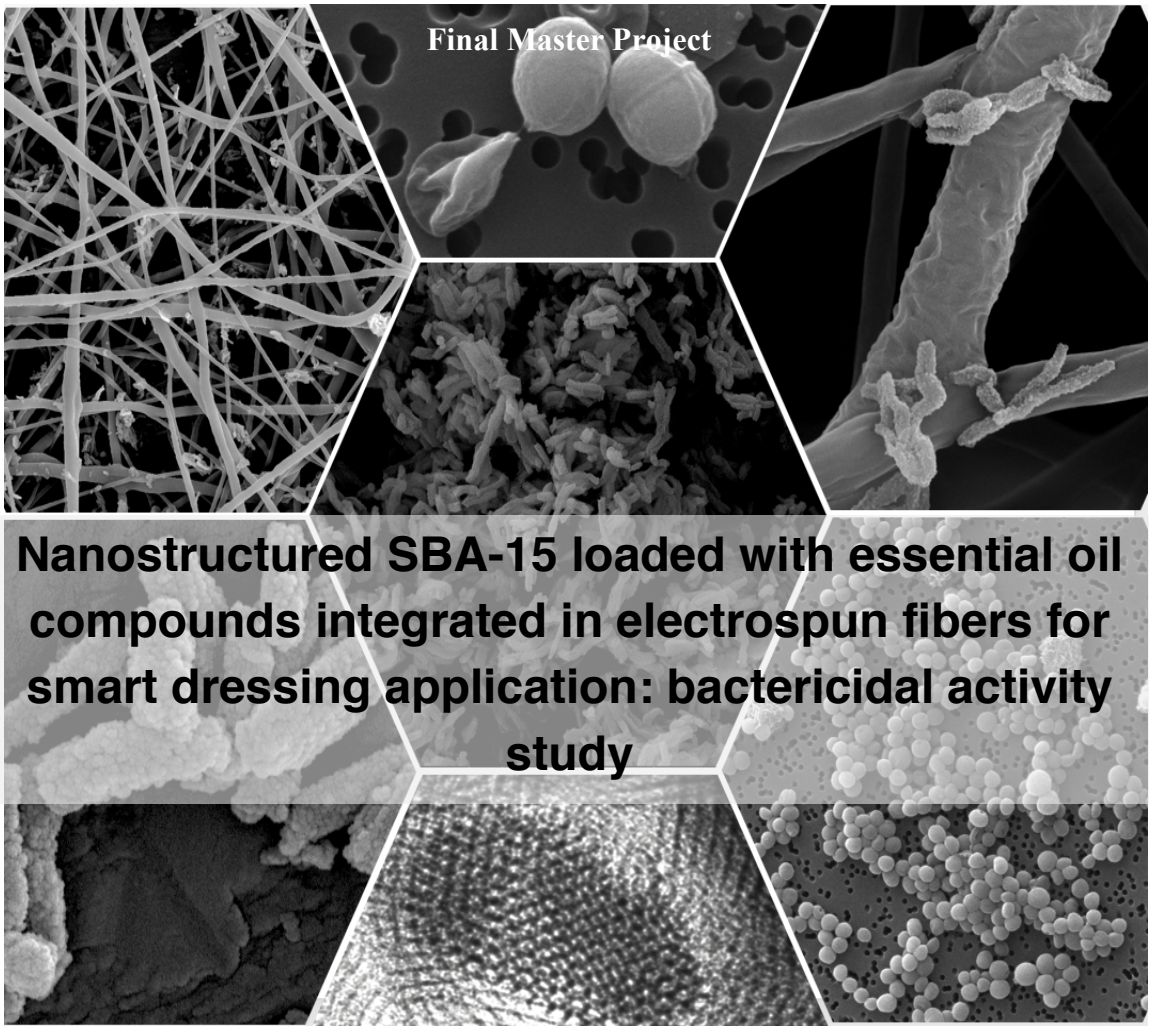

Nanostructured SBA-15 loaded with essential oil compounds integrated in electrospun fibers for smart dressing application: bactericidal activity study

Hellen Elizondo Castillo

Supervisor: Dra. Silvia Irusta Alderete

nanostructured films & particles

June 2017

micitt

ABSTRACT

The treatment of skin and soft tissue infections (SSTI) represent a significant financial and clinical treatment concern. Therefore, it is important to develop novel strategies to combat the SSTI and the associated microorganisms, which are the main obstacle in healing processes.

In this study, an essential oil compound (EOC) loaded nanostructured SBA-15, with bactericidal action against *Staphylococcus aureus* was developed. Additionally, these EOC loaded SBA-15 particles were attached to electrospun polycaprolactone (PCL) fibers. In this system, silica support behaves as EOC carrier, while the PCL fibrous structure provides a matrix suitable for wound dressing application.

The antimicrobial effect of essential oil compounds was evaluated by the Minimum Inhibitory Concentration (MIC) and Minimum Bactericidal Concentration (MBC) *in vitro* determination. Carvacrol and thymol exhibited the higher bactericidal activity with MBC values of 0.3 mg/mL, followed by cinnamaldehyde with 0.5 mg/mL.

Dispersed rod-shaped SBA-15 particles have been synthesized, with an external diameter of 138 nm, a length of 563 nm and pore volume of 1.5 cm^3/g. Then, carvacrol, thymol, or cinnamaldehyde were loaded into SBA-15 by incipient wetness impregnation method with a highly concentrated EOC ethyl acetate solution, yielding loading efficiencies (LE) as high as 256.0 % for carvacrol, 267.5 % for thymol, and 205.7% for cinnamaldehyde.

The release of loaded EOC was sustained for the first 48 h, with 68% and 64 % release for carvacrol and thymol composites, respectively. EOC loaded SBA-15 showed a strong bactericidal effect on *S. aureus*. Compared with pure compound, the nanocomposite resulted in the enhancement of bactericidal activity of tested EOC, due to the mesoporous materials contribute to the solubility improvement of poorly water soluble compounds and the sustained release profile.

Furthermore, the attachment of thymol SBA-15 loaded nanocomposite on biocompatible PLC fibers via electrospinning, was confirmed by SEM. Images showed well distributed and dispersed rods on fibers surface.

This work has resulted in the formation of SBA-15 rod-shaped carriers loaded with EOC with enhanced bactericidal properties, as a promising composite system capable of being attached to biopolymer fibers surface, to be used as a wound dressing with antimicrobial properties in order to develop more efficient dressings for wound healing.

INDEX

ABBREVIATION LIST

ATR-FTIR	Attenuated Total Reflectance- Fourier Transform Infrared Spectroscopy
BET	Brunauer, Emmett and Teller
CIN	Cinnamaldehyde
CRV	Carvacrol
EOC	Essential Oil Compound
EOC/SBA	Essential oil compound loaded SBA-15
GC-MS	Gas chromatography- Mass Spectroscopy
IW	Incipient Wetness Impregnation Method
LE	Loading efficiency
MBC	Minimum Bactericidal Concentration
MIC	Minimum Inhibitory Concentration
PBS	Phosphate Buffered Saline
PCL	Polycaprolactone
SBA-15	Santa Barbara Amorphous-15
SEM	Scanning Electron Microscopy
SMP	Silica mesoporous
SSTI	Skin and soft tissue infection
TEM	Transmission Electron Microscopy
TGA	Thermogravimetric Analysis
THY	Thymol
TSB	Tryptic Soy Broth
UPLC	Ultra Performance Liquid Chromatography
VI	Vacuum Impregnation Method
XRD	X-Ray Diffraction

INTRODUCTION

Skin is the largest mechanical barrier in the body. It forms an effective barrier between the external environment and the organism, protecting the body from water loss, pathogens, and harmful assaults. Skin protection may be compromised by injuries such as burns, ulcers, trauma or wounds [1]. The skin and soft tissue infections involve microbial occupation originated from the accumulation of the fluid at the wound site, spoiling the healing process. Regarding their severity, SSTIs commonly represent a clinical treatment concern. In this scenario, an important percentage of hospitalized patients that exhibit SSTIs increasing the economic burden of health care systems, concerning resources, staff time and treatments [2, 3]. It has been determined that non-healing wounds in the United States stand for the 2% of the population, being the associate cost of caring for these injuries more than $50 billion per year, that is ten times higher than the annual budget of the World Health Organization [4]. For this reason, the wound care has acquired global attention to provide a proper and favorable atmosphere for the recovery process. The incorporation of antimicrobial agents as a requirement to prevent infections at the wound site, the enhancement of the wound healing efficiency, the reduction of medical costs and the improvement of the patient's quality of life have become in main issues to achieve an adequate wound healing [5].

Wound dressings are protective barriers used to sustain the healing process. In comparison to usual bandages, electrospun fibers may act as an optimal support for healing. Consequently, it has been an increased interest in the development of electrospun nanofiber mats, in order to accelerate and improve the wound healing and prevent bacterial infections [6]. Electrospinning is a simple and versatile fabrication technique to generate micro/nanofibers, through the application of a high voltage electrical field to a polymer droplet at the tip of an injection needle. Antibacterial drug loaded nanofibers can easily be produced with natural and synthetic polymers [7].

Previous authors have reported different studies in which drug delivery electrospun nano-dressings have been developed by using a wide variety of biocompatible materials such as cellulose, polycaprolactone (PCL) or poly(vinyl acetate), together with antimicrobials compounds [7].

Diverse methods of loading drugs into the fibers have been reported, for instance, the drug immobilization, drug adsorption or drug mixed with the polymer solution [8]. However,

the attention to the nanofibers decorated with drug loaded nanoparticles is a growing field. This system may yield a particular drug release profile along with the high drug loading capacity, improving the healing environment. Even though the use of loaded nanoparticles for fiber decoration has been described, the implementation of drug loaded mesoporous materials to embed fibers is incipient [6, 8].

The development of nanoscale carriers for drug delivery is an emerging approach. For this reason, nanotechnology is a coming up field in medicine with significant therapeutic benefits. The nano-encapsulation contributes to overcoming hydrophobic and volatile drawbacks of commonly used drugs, by increasing the physical stability, decreasing volatility and toxicity, and protecting them from environmental interactions, which enhances the bioactivity that results in an improvement of the patient compliance and convenience [9]. In this field, the use of high surface area mesoporous materials as EOC nanocarriers is a coming up approach, because of being systems with a large loading capacity, providing an active compound protection and compound solubility improvement [10].

Mesoporous silica materials are silicon dioxide structures with pores between 2-50 nm [11]. Their synthesis is based on the supramolecular self-assembly of surfactants and the formation of a hexagonal array of cylindrical micelles produced by these amphiphilic molecules. The incorporation of the silicate precursor produces inorganic walls between the micelles, developing a template framework. After the sol-gel polycondensation, the surfactant is removed through a calcination process at high temperature, giving rise to the porous network [12]. Figure 1 shows a general scheme of mesoporous materials formation by structure directing agents, by cooperative self-assembly [13].

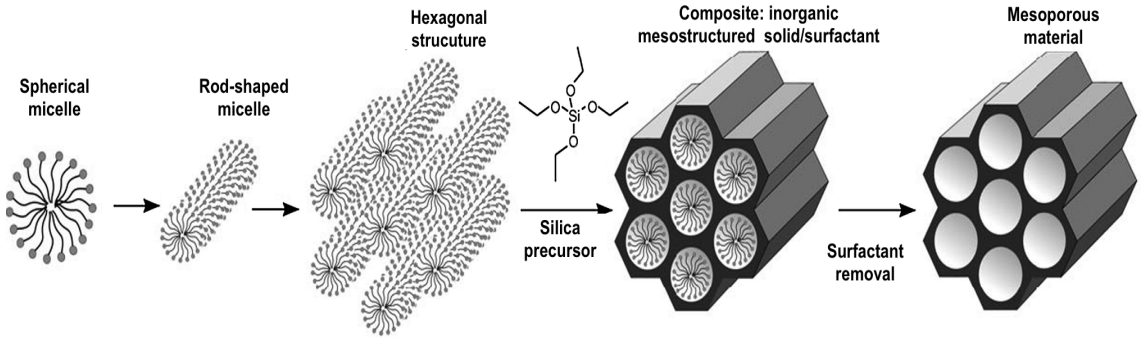

Figure 1. Representation of mesoporous silica materials through surfactant structure directing agents, by cooperative liquid-crystal, adapted from Hoffman *et al.* [13]

Santa Barbara amorphous-15 (SBA-15) exhibits two-dimensional hexagonal structures (*p6mm*), and a highly ordered hexagonal array of cylindrical mesopores generally between 6-10 nm [14, 15]. It possesses uniform and controllable pore size, a thick pore wall, high pore volume and surface area (> 600 m^2/g). Moreover, it has high hydrothermal, thermal and mechanical stability [16]. Silica support can be synthesized in a variety of morphologies such fibers, spheres, platelets or rods by modifications of synthetic parameters such as stirring, acidity and reaction time. The rodlike structure attracts the attention due to the small dimensions, resulting in short diffusion paths, fast absorption and fast mass transfer [17].

Mesoporous materials (MSP) and specifically the SBA-15 have found their application in chemistry and material science fields, including absorption of volatile organic compounds, catalysts, and metal encapsulation. An arising application is their use as drug nanocarriers regarding their remarkable properties such as i) the high loading capacity, ii) the tunable pore size and well-defined structure, iii) the two functional surfaces, iv) the stability against chemical, biological and thermal attack, v) the safe composition, vi) their biocompatibility, vii) the improvement of the dissolution of poorly water-soluble molecules, and viii) the protection of their load against degradation [11].

The most important human virulent pathogen with large public health concerns is S*taphylococcus aureus* (*S. aureus*). It is responsible for a broad spectrum of clinical infections, ranging from skin and soft tissue infections to life-threatening systemic infections, causing approximately 20 000 deaths per year [18, 19]. *S. aureus*, are gram-positive cocci with a permeable wall, the diameter between 0.5-1.0 μm and occurs in grape-like clusters [3].

Unfortunately, due to the overuse and abuse of antimicrobial agents, the multidrug resistance rises with the reduction in the efficacy of current therapies, resulting in thousands of deaths [9]. *S. aureus* is the most frequently occurring pathogen from SSTIs with Methicillin Resistance (MRSA) with the greatest concern to face therapy in the outpatient setting. This issue now is recognized as an emerging global challenge [1]. Nowadays, there are new medical practices implanted so as to stand up to MRSA, for example preventing infections, vaccination and better control over health care facilities. Nevertheless, novel alternative antimicrobials are required. In this scenario, the use of essential oils (EO) as antimicrobials is leading to a promising alternative for drug resistance [3].

Essential oils are complex natural mixtures of volatile secondary metabolites isolated from plants. Relevant functional groups of EO, including aldehydes, alcohols, acids, and

phenols, play an appropriate role as antimicrobials. Among them, phenols and aldehydes exhibited the major bactericidal activity [9]. For example, the antibacterial activity attributed to compounds such as carvacrol, thymol, and eugenol is due to the phenolic hydroxyl group presented in their structures [9, 20]. Although the bactericidal mechanism of essential oil compounds (EOC) remain unclear, there is evidence of physicochemical and physiological changes in bacteria structure, which suggests that their antimicrobial mechanism is mediated through the breakdown of the cytoplasmic cell membrane [21, 22]. EOCs are small molecules (< 2 nm) that could penetrate quickly through bacteria wall. Besides, the hydrophobicity and lipophilic nature of EOC allows them to easily interact with fatty acids of the dense microbial cell membrane [9].

Nowadays, the interest in natural antimicrobials is growing due to their availability, better biodegradability, and fewer side effects. And most important, even when they have been used for long time, there is no evidence of microbial resistance. Besides, it is well-known that some secondary metabolites also display antioxidant, anti-inflammatory, insecticidal, anticancer and anti-allergic properties [23, 24]. However, essential oil compounds exhibit technological drawbacks associated with natural products such as reactivity, poor water solubility, and high volatility, which decrease their biological effect and limit their applications [25].

The use of EOC involves the interaction with hydrophobic compounds. With this regard, it has been widely reported that the periodic structure of SMP facilitates the dissolution of poorly water soluble bioactive compounds commonly used in therapeutics. Through the breakdown of the intermolecular interactions of drug molecules, the dissolution is enhanced [10, 26]. The literature reported successful studies of hydrophobic drug encapsulation into SMP, for instance, gentamicin, diazepam, and indomethacin [14, 10]. Nevertheless, only a few publications of EOC encapsulation within SBA-15 pores were founded, i.e. studies performed by J. Lillie [3], and Bernardos *et al*. [25].

Different drug loading methods into SBA-15 nanoparticles have been reported. Conventional techniques include the absorption from an organic solution followed by filtration, vacuum impregnation, and slow solvent evaporation [11]. To obtain the higher amount of bioactive molecules into the pores, the loading method selection is a fundamental step, especially when hydrophobic compounds are employed. Factors such as molecule and pore size, specific pore volume, compound solubility, solution viscosity and temperature, should be considered. Figure 2 shows a representation of loading methods.

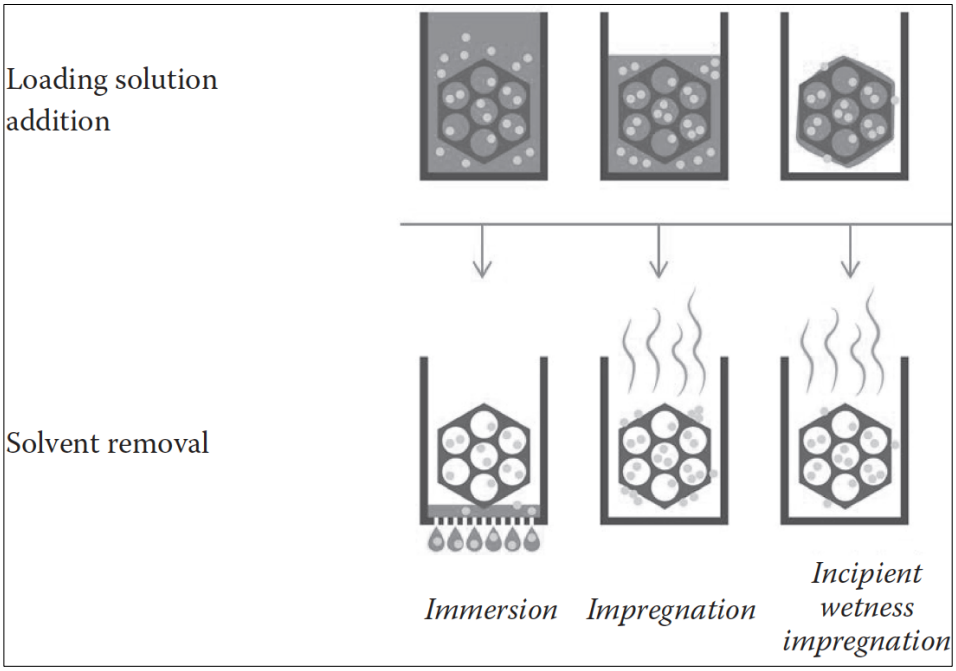

Figure 2. Scheme of different loading methods [11].

The most convenient approach is based on void space filling, which is called incipient wetness (IW) impregnation. IW method takes advantage of the large pore volume of the material, in which a precise amount of highly concentrated compound solution fills the void space [26]. The vacuum impregnation (VI) method comprises the compound addition to a closed system, after being exposed to high temperature under reduced pressure to eliminate the water from the pores [27].

The mesoporous silica materials are promising drug delivery systems, due to the release modulation of adsorbed EOC to the aqueous media, representing a bright approach towards the reduction of burst release providing a controlled compound delivery [9].

This research involves the *in vitro* evaluation of bactericidal activity of EOC against *S. aureus*, bacteria commonly associated with SSTIs. Carvacrol, thymol, and cinnamaldehyde were encapsulated into synthesized mesoporous materials (SBA-15). Thymol/SBA-15 nanocomposite was attached to biocompatible fibers to be used as wound dressing with bactericidal properties.

OBJECTIVES

The purpose of this Final Master Project is to obtain SBA-15 particles loaded with EOCs with bactericidal properties to be used as electrospun fiber decoration in a wound dressing material.

The proposed specific objectives to achieve this primary goal are the following:

1. Identification of EOCs with optimal bactericidal properties against S. aureus, a bacteria strain commonly associated to wound infections: EOCs selection for further studies was based on their performance according to the MIC and MBC results. The EOCs under study and their chemical structures are shown in Figure 3.

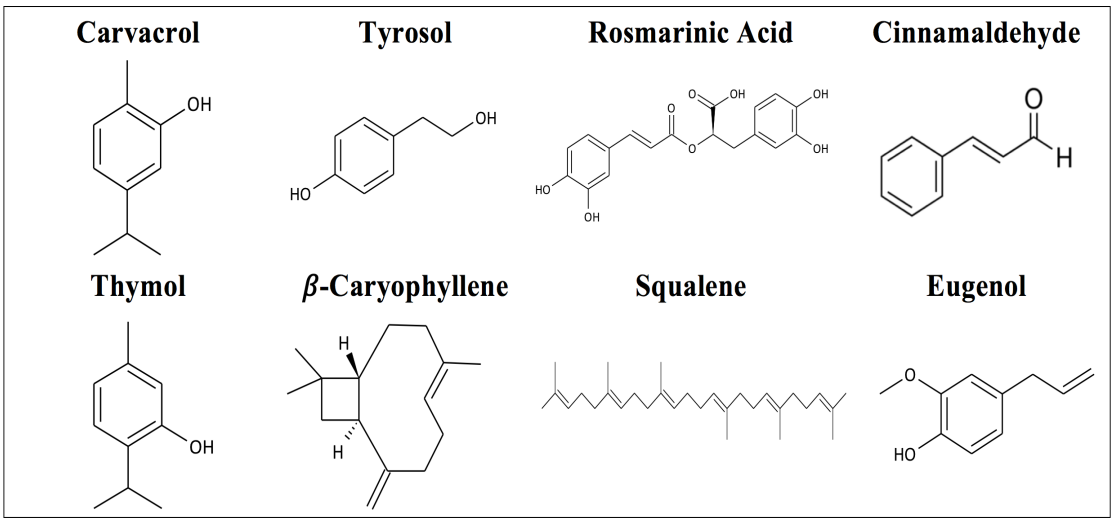

Figure 3. Essential oils active compounds employed in MIC and MBC assays

2. EOC loading into synthesized SBA-15 rod-shaped particles and compounds release study: the SBA-15 channels (2-50 nm diameter) can be filled with different compounds, in fact many hydrophobic drugs have been loaded inside mesoporous material [10]. Nevertheless, there are few studies related to the EOC. To fulfill this objective, different loading methods and experimental parameters were evaluated to reach the highest oil amount inside rod channels. The particles were independently loaded with the three EOCs which exhibited the higher bactericidal effect against *S. aureus*, by using the best method and conditions. The release profile of EOCs in PBS was studied.

3. Determination of the bactericidal effect of SBA-15 loaded particles: To achieve this objective, the bactericidal effect of the SBA-15 loaded particles with the three EOCs with higher bactericidal effect against *S. aureus* was determined.

4. Development of PCL fibers decorated with SBA-15 rod-shaped nanoparticles: As a proof of concept, the suitability of SBA-15 materials to be deposited on PCL fibers were tested. Hybrid fiber assembly was performed by using the electrospinning technique.

EXPERIMENTAL METHODS

Techniques and materials utilized in this project are described in Annex A.

Experimental methods

Methods developed during this project are summarized here. The detailed protocols and conditions are described in Annex A.2.

- **Synthesis of rod-shaped mesoporous silica support (SBA-15):** SBA-15 was prepared according to the hydrothermal synthesis method reported by Johansson *et al.* [28]. The resultant material was characterized by Nitrogen adsorption-desorption technique, ATR-FTIR, TGA, TEM, SEM and XRD.
- **Essential oil compounds loading and method optimization:** Two EOC loading methods were evaluated, the IW impregnation and VI. Experimental parameters were modified to assess their influence in %LE (Table A.2.1). With the selected method, nanocomposites were impregnated with a highly-concentrated THY, CAR or CIN solution, for 1 h, washed with distilled water and filtered. Loading efficiency was determined by TGA measurements.
- **Essential oil compound release profile:** loaded samples were dispersed in PBS and placed in a Slide-A-Lyzer® MINI dialysis device to determine the release profile of EOC from SBA-15 support.
- **EOC organic extraction:** Nanocomposites were treated with organic solvents during 24 h, the solution was analyzed by GC-MS to confirm the EOC loading into the SBA-15.
- **Thymol loaded SBA-15 deposited on PCL fibers:** the double nozzle technique produced PCL fibers decorated with SBA-15. Particles were added to fibers surface using suspensions with different SBA-15 concentrations. A field test was performed with thymol loaded particles. Samples were characterized by SEM
- **Bactericidal activity of EOCs and loaded nanoparticles:** MIC and MBC of the seven EOCs were evaluated in *S. aureus* by using the broth dilution assay method.

Bactericidal activity of loaded nanoparticles was tested by the same method at different EOC concentrations based on TGA analysis, using empty SBA-15 as a growth control.

RESULTS AND DISCUSSION

- **Identification of EOCs with optimal bactericidal properties against *S. aureus*, a bacterial strain commonly associated to wound infections**

Staphylococcus aureus are gram-positive bacteria generally present in skin infections [7]. There are several methods to evaluate the antimicrobial activity of EOCs, some of them include disc diffusion, well diffusion, agar dilution and broth dilution. MIC and MBC are values employed to analyze the bactericidal performance of compounds or molecules. MIC is defined as, the minimum concentration that produces a 90% reduction in the growth of microbial colonies, and MBC represents the minimum concentration that produces at least a 99.9% reduction of microbial cells [29]. In this section, these concentrations were determined for the compounds cited in Figure 3. Experimental results are presented in Table 1.

Table 1. MIC and MBC results for tested compounds on *S. aureus*.

Essential oil compound	MIC (mg/mL)	MBC (mg/mL)
Carvacrol	0.2	0.3
Thymol	0.2	0.3
Cinnamaldehyde	0.4	0.5
Tyrosol	1.0	4.0
Eugenol	1.3	1.5
Rosmarinic Acid	2.5	> 4.0
Squalene	> 4.0	> 4.0
β- Caryophilline	> 4.0	> 4.0

Bacteria control results are showed in Table B.1.1 (Annex B). Chlorhexidine was selected as negative control owing to its quicker kill rate, the broad-spectrum biocide effectiveness as well as due to its wide use in the clinic [30]. Results from Tween control did not exhibit influence over bacteria growth.

Among tested compounds, carvacrol (CRV) and thymol (THY) showed the higher antimicrobial activity showing the lowest MIC values (0.2 mg/mL), close to the chlorhexidine negative control. Both compounds displayed a total growth inhibition at 0.3 mg/mL. These results are similar to those published by Lang-Hong *et al.* reporting a MIC value of 0.3 mg/mL for carvacrol [31]. In this sense, Burt stated a MIC value for thymol in the range of 0.14-0.22 mg/mL [32].

Cinnamaldehyde (CIN) was the third compound that exerted a high ability to inhibit bacteria growth, displaying a MIC value of 0.4 mg/mL, which is similar to previous studies that reported a MIC value of 0.25 mg/mL for this compound [33].

Eugenol and tyrosol showed lower antibacterial activity, with MIC values of 1.0 and 1.2 mg/mL, respectively. The MBC obtained for eugenol agrees with those reported by Ananda *et al.* (1.4 mg/mL) [34]. Rosmarinic acid, squalene, and caryophyllene showed very low antibacterial activity. They did not present significant differences to the positive control (bacteria growth of 10^9 CFU/mL, Table B.1.1) at the highest concentration tested (4 mg/mL). Concentrations above 4 mg/mL were not measured due to nanoparticle encapsulation drawbacks and efficiency.

Results from statistical analysis determined a significant difference of MIC and MBC values against the control sample, showing the clear bactericidal activity of the selected EOCs. Table B.1.2 (Annex B) shows bacteria concentration at MIC values and the standard deviation for all tested compounds. Figure B.1 depicts the comparison among different active EOCs regarding MIC values.

Given these results, three compounds were selected for further assays: CRV, CIN, and THY owing to their better antibacterial activity. As mentioned before, the bactericidal behavior is associated with their chemical structure. In Gram-positive bacteria, terpenes like CRV and THY produce damage in membrane integrity, with the consequent affectation in pH homeostasis of inorganic ions equilibrium [22]. On the other hand, Shang-Tzen *et al.* stated that its chemical structure also influences CIN antibacterial properties. Some features like conjugated double bond, long chain outside the ring, and the aldehyde group provide bactericidal behavior [33]. To mechanism confirmation, bacteria SEM images were obtained after being exposed to MIC and MBC concentrations of CRV, CIN, and THY for 24 h. Figure 4 displays the acquired images after treatment with THY, while in Figure B.1.2 (Annex B) bacteria images treated with CRV and CIN are presented.

The untreated bacteria showed the characteristic round shape morphology without any structural changes, while treated bacteria in all cases became deformed and wrinkled, as SEM images show. According to the literature, there are different suggested theories about the antimicrobial mechanism. In general, for Gram-positive bacteria, oil compounds would disturb the equilibrium of bacteria components, being reflected in the detriment of motive force, depletion of intracellular adenosine triphosphate (ATP) pool, and the leakage of internal substances such as nucleic acids or amino acids. Owing to the internal disequilibrium,

bacteria wall and membrane are disrupted as the SEM micrographs confirmed showing a deflated or collapsed structure [22, 35].

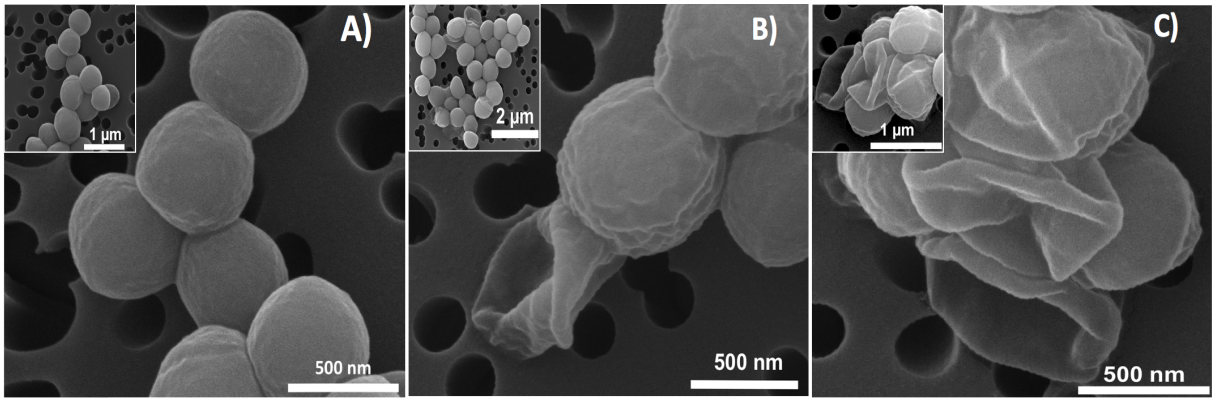

Figure 4. SEM micrographs of *S. aureus*. **A)** untreated bacteria (positive control). **B)** Treated bacteria with THY at 0.2 mg/mL (MIC). **C)** Treated bacteria with THY at 0.3 mg/mL (MBC).

- **EOC loading into synthesized SBA-15 rod-shaped particles and compounds release study**

SBA-15 rod-shaped particles were synthesized according to the method explained in the experimental section.

Figure 5 shows the morphological characterization of SBA-15 nanoparticles from TEM and SEM analysis. Both images confirmed the rodlike shape and illustrated the presence of internal parallel channels oriented along the material axis, as well as some external connections between the rods which are also reported as curved bridges [15]. Inset in Figure 5.A provides a view of the hexagonal faceted structure. Frequency histograms of SBA-15 nanoparticle obtained by ImageJ from SEM images are shown in Figure C.1.1 (Annex C). The mean external diameter of rod-shaped nanoparticle was 138±30 nm, and the mean length 563±100 nm.

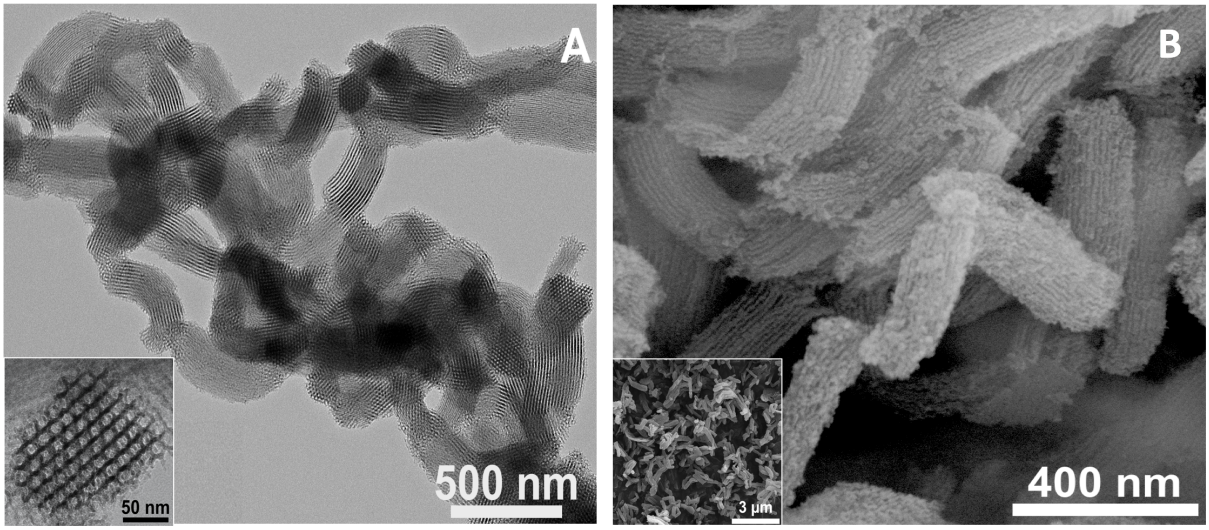

Figure 5. Morphological analysis of SBA-15 rodlike nanoparticles. **A)** TEM micrograph. **B)** SEM micrograph

Figure 6 depicts further SBA-15 characterization results from XRD patterns and Nitrogen adsorption-desorption analysis. The highly ordered hexagonal structure is evident in the X-Ray Diffraction pattern (Figure 6.A) with the presence of three typical diffraction peaks with a maximum at 2θ: 0.6, 1.0 and 1.2 which correspond to (100), (110) and (200) reflections for *p6mm* space group [36]. According to Pikus *et al*. these peaks at low angles are due to the presence of large ordered pores [37].

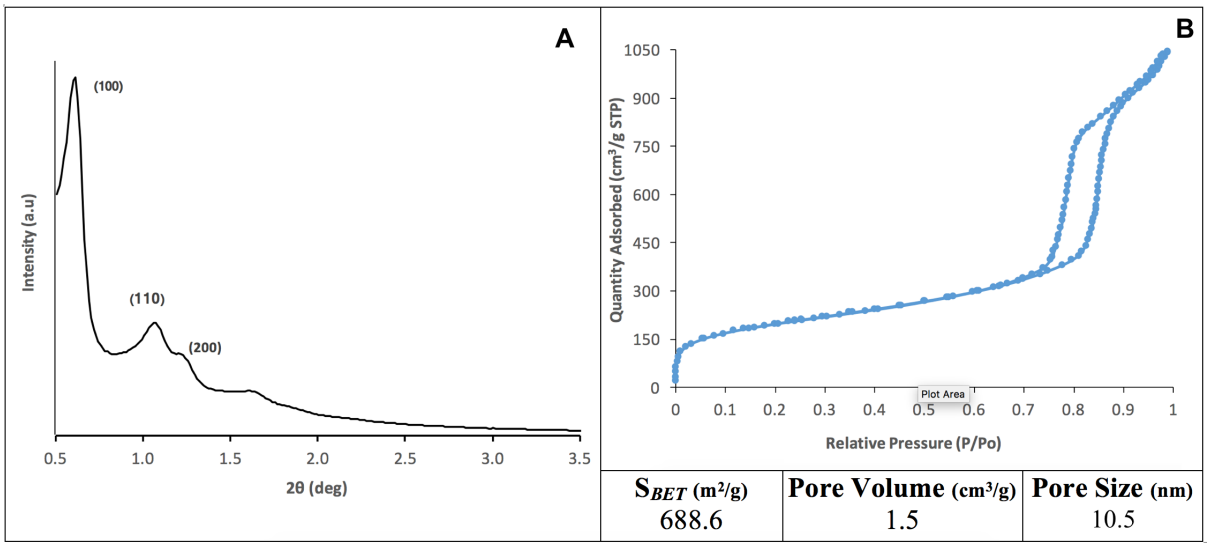

S_{BET} (m²/g)	Pore Volume (cm³/g)	Pore Size (nm)
688.6	1.5	10.5

Figure 6. Synthetized SBA-15 characterization **A)** Small Angle XRD diagram. **B)** N_2 sorption isotherm. Inset material properties

Figure 6.B shows a Nitrogen adsorption-desorption isotherm for SBA-15. A typical type IV curve of adsorption isotherm with an H_1 hysteresis loop is observed, which is associated with the presence of cylindrical and hexagonally ordered mesopores. The relative

pressure position of the hysteresis loop ranging from 0.7 to 0.9 verifies this structural porous characteristic. Moreover, BET surface area fitted with the characteristic values for this type of material [28]. Additionally, the pore size distribution is a narrow sharp peak centered at 10.5 nm, which confirmed a pore size in the range of 8-15 nm (Figure C.1.2, Annex C)) [15]. Lastly, from N_2 adsorption-desorption analysis, pore volume determined the theoretical capacity of the material to entrap the EOCs.

Thermogravimetric analysis (Figure C.1.3) demonstrated the overall surfactant removal after calcination process, owing to the absence of thermal degradation steps. The residue after 525 °C is related to SBA-15 material.

Optimization of loading method

In order to achieve the highest amount of EOC loaded into SBA-15 pores, two loading methods were carried out: vacuum impregnation and incipient wetness impregnation. Moreover, the influence of some experimental parameters on the loading efficiency was evaluated. The conditions tested were: EOC concentration (pure or diluted), impregnation time, EOC quantity (1x or 5x), solvent, and final wash. In this section, CRV was employed as a model compound for the method selection. Thermogravimetric measurements quantified the amount of loaded compound.

Table 2 details the influence of variations in impregnation time, EOC concentration and amount of added compound over the loading efficiency. As it can be observed, comparing samples ID2 and ID3 a higher loading was obtained when the impregnation time was increased, samples IP3 and IP4 exhibited the same behavior when the pure compound was employed. Therefore, the higher the contact time, the higher the loading efficiency achieved.

Table 2. Carvacrol loaded SBA-15 by incipient wetness impregnation method

Sample	Quantity *	Concentration	Impregnation time (h)	%LE***
ID2	1x	Diluted**	3.5	54.4
ID3	1x	Diluted**	1.0	44.6
IP3	5x	Pure	24.0	432.2
IP4	5x	Pure	1.0	64.2
ID4	5x	Diluted**	1.0	256.0

*EOC amount added referred to the theoretical capacity

**Solvent: Ethyl acetate

*** From TGA results

The use of the theoretical quantity of CRV (1x) referred to the support pore volume, resulted in low loading efficiency (samples ID2 and ID3), obtaining %LE up to 54.4%. However, the addition of five times the theoretical pore capacity (5x) (sample ID4) rendered in a %LE of 256%. With these results, we can infer that EOC molecules were inside the pores as well as, on the rods surface.

When the pure compound was employed (sample IP4), it resulted in a lower EOC loading than in sample ID4, in which CRV diluted in ethyl acetate was used for impregnation. This implied that the use of a highly-concentrated oil dissolution rendered a better compound loading than the pure compound. It has been reported that the solution viscosity is a factor that should be considered when encapsulation of molecules inside mesoporous materials is intended. A highly viscous solution may interfere with the material manipulation, thus the ineffective compound adsorption within the pores [11]. The influence of pure compound viscosity and the amount of EOC added is represented in Figure 7. The material did not get totally wet with the theoretical amount (1x) and then not all the MSP support was in contact with the EOC, with the addition of more amount of EOC the impregnation is improved.

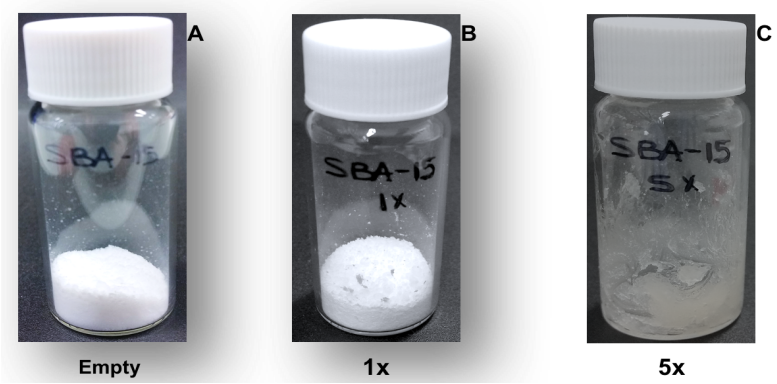

Figure 7. SBA-15 impregnated with a different concentration of EOC. A) SBA-15 empty B) SBA-15 with theoretical EOC amount (1x). C) SBA-15 with EOC excess (5x).

On the other hand, the impregnation of SBA-15 with an excess (5x) of pure carvacrol during 24 h (sample IP3), resulted in a remarkable EOC adsorption in the mesoporous support, above 400%. However, due to the previously mentioned inconveniences related to the viscosity, the uniform distribution of the EOC in the support cannot be assured, besides the time required to achieve high loading was 24 h, as consequence this method was discarded.

Figure C.2.1 (Annex C.2) displays the TGA thermograms of loaded samples. As mentioned before, the loadings efficiency reported in Table 2 were determined from these

measurements. From these curves, it is clear that the higher loading was achieved for sample ID4 when impregnation time of 1 h was employed with the diluted compound.

Table 3 compares incipient wetness impregnation with vacuum impregnation results. Even when the vacuum method involved an impregnation time of 15 h (sample VI(D)), the loading efficiency was only 18.8%. This result could be influenced by the lack of stirring that avoided a homogeneous sample distribution during the impregnation step.

Table 3. Carvacrol loaded SBA-15 by incipient wetness impregnation method, and vacuum impregnation method. CRV diluted in ethyl acetate

Sample	Method	Quantity *	Impregnation time (h)	%LE***
VI(D)	Vacuum impregnation	1x	15	18.8
ID3	Incipient wetness	1x	1.0	44.6

*EOC amount added referred to the theoretical capacity *** From TGA results

The thermograms associated with the samples under discussion can be seen in Figure 8. From vacuum impregnation method, sample (VI (D)) shows an overall degradation percentage of 20%. The first degradation step is attributed to EOC that remains on SBA-15 rods surface. The second decomposition corresponds to EOC inside the SBA-15 mesopores. Sample ID3 exhibited the same behavior with a higher percentage of mass loss (39%).

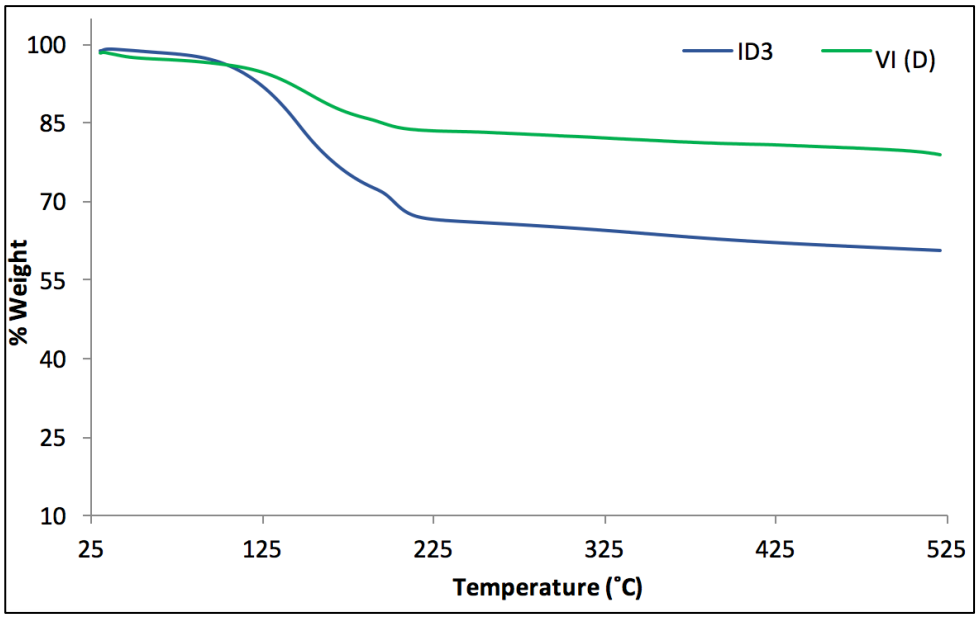

Figure 8. Thermogravimetric curves for SBA-15 samples loaded with carvacrol by incipient wetness impregnation (ID3), and vacuum impregnation (VI(D)).

Additionally to the exposed data, the vacuum impregnation method was a time and energy consuming process. Based on these results, the use of this loading method was discarded.

Supplementary experiments with experimental variations exhibited lower loading efficiency than the above described. Table C.2.1 (Annex C.2) bring together the main results, while Figure C.2.2 presents the resulting thermograms. The use of ethanol for the final wash promoted the removal of the compound located on the support surface and inside the pores, owing to EOC solubility. Moreover, for this project, an additional oil loading on the material surface was an advantage in order to provide a higher EOC available to interact with the bacteria.

After studying the different loading methods and parameters, for the next CRV, THY and CIN loadings into SBA-15, experimental conditions selected were those followed in the synthesis of sample ID4. Briefly, by incipient wetness impregnation method, compound dilution with ethyl acetate, 1 h of impregnation under stirring, and water for final wash. The selection was made by considering the loading efficiency, time and energy convenience, and material composition. Onwards, nanocomposite materials will be denoted as EOC/SBA (CRV/SBA, THY/SBA, CIN/SBA)

The EOC loaded materials were obtained by impregnation of SMP supports, with a diluted-1x and a saturated-5x EOC solution (1x corresponds to the SBA-15 pore volume). Characterization results for CRV/SBA and CIN/SBA nanocomposites are shown in Figures C.2.3 and C.2.4 (Annex C.2).

Besides, the quantification of loaded compounds into SBA-15 through thermogravimetric analysis, organic compound extraction was carried out. Figure 9 illustrates the thermal degradation of THY/SBA nanocomposite. Sample 1x shows a mass loss of 45%, and sample 5x a degradation percentage of 80%.

Both samples presented a notable first weight loss between 80-160 °C, which is attributed to the decomposition of thymol from SBA-15 surface and inside the pores. A second small event in the range of 160-215 °C corresponds to the degradation of thymol inside the interconnections and EOC that remains inside the pores. The higher degradation temperature of the loaded compound than the free compound can be attributed to the mesoporous silica material. This support increases the EOC thermal stability since thymol decomposition according to Figure C.2.5.B is in the range of 55-128 °C. The remaining mass at the end of the thermogram is associated with the siliceous material.

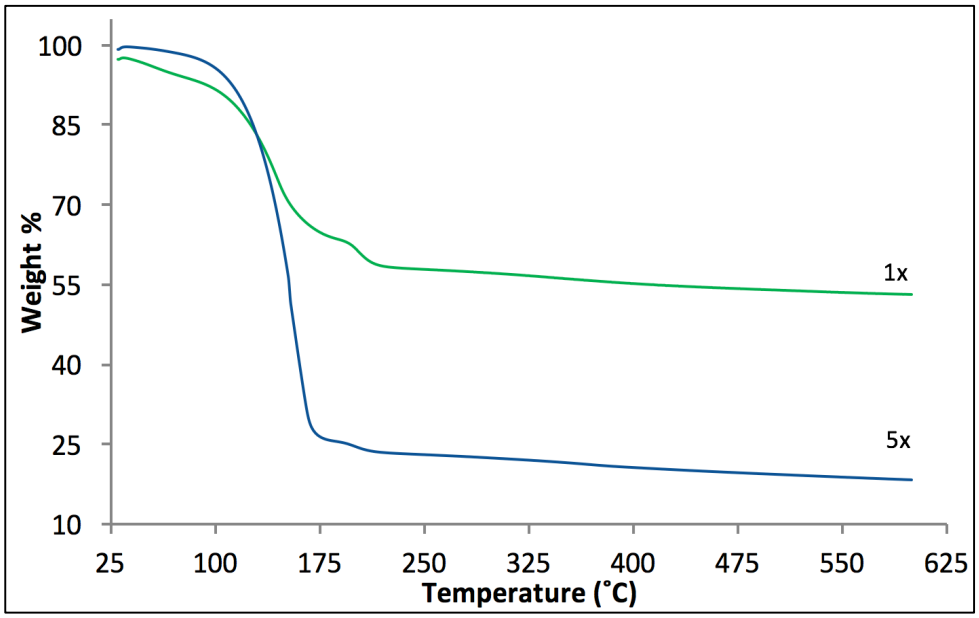

Figure 9. TGA diagrams of THY/SBA loaded particles for the diluted-1x and a saturated-5x EOC concentration.

Samples of CRV/SBA (Figure C.2.3.A) and CIN/SBA (Figure C.2.4.A), exhibited the same behavior than thymol composite. A total weight loss of 40% for CRV/SBA and 36% for CIN/SBA in 1x samples. For 5x samples, degradation percentages of 79% and 77% for CRV and CIN loaded materials respectively, were obtained. Moreover, similarly to THY/SBA nanocomposite, two mass losses events were observed together with the increase of thermal stability of EOC promoted by silica support compared to the pure free compound (Figures C.2.5. A, C).

Table 4 depicts the amount of compound loaded into the SBA-15 sample, determined by TGA and organic extraction. In all cases, when theoretical EOC volume was used (1x), a loading efficiency equal or below 56.5% was achieved.

On the other hand, the increase in the EOC quantity (5x) yielded an increment of loaded material, which would infer the completed pore filling. The loading efficiency above 100% confirms these results and suggests the presence of an external deposition of EOC on SBA-15 surface.

Loading results are lower for the organic extraction quantification method in comparison to those from TGA. These variations could be associated with differences between techniques (TGA and GC-MS), and extraction process. Regarding extraction data, results could be influenced by the organic solvent employed. The solvents utilized would not extract all the EOC from inside the pores, leading to a lower mass quantification. Regarding

TGA analysis, all samples were previously dried before the measurements to avoid mass losses assigned to water content or humidity. Nevertheless, a small amount of remaining water could interfere in mass losses quantification assigned to the loaded compound.

Table 4. EOC/SBA-15 loaded particles quantified by thermogravimetric analysis and organic extraction

Loaded EOC Particles	EOC quantity	%LE	
		TGA	Organic Extraction
CIN/SBA	1x	35.6	*
	5x	205.7	*
CRV/SBA	1x	44.6	12.4
	5x	256.0	215.3
TIM/SBA	1x	56.5	23.3
	5x	267.5	233.9

* Results from CIN quantification from organic extraction are not representative

Concerning to CIN/SBA sample, the GC-MS chromatogram showed an unusual result (Figure C.2.6, in Annex C), displaying two new peaks corresponding to *cis*-cinnamaldehyde and a benzaldehyde molecules. Since only *trans*-cinnamaldehyde peak was considered for the chromatographic quantification method, this technique cannot be used for this compound determination.

Cinnamaldehyde decomposition was previously studied by Friedman *et al*., who stated that for the pure compound in the presence of oxygen at a fairly low temperature, the decrease of CIN content was accompanied by the appearance of benzaldehyde, and demonstrated a higher degradation with temperature increments [38]. In our experiments, the organic extraction was performed under stirring for 24 h, in the presence of oxygen and organic solvents, which could promote the compound degradation yielding benzaldehyde, as it is shown in GC-MS chromatogram.

According to the nanostructure morphological analysis, carried out by SEM Figures 10.B, C.2.3.B, and C.2.4.B), the presence of EOCs on the surface of SBA-15 in all the nanocomposites was confirmed when it was compared to the empty particles (Figure 10.A). Two main differences can be noted, the lumps in the surface and the lack of visible strips that correspond to the internal channels.

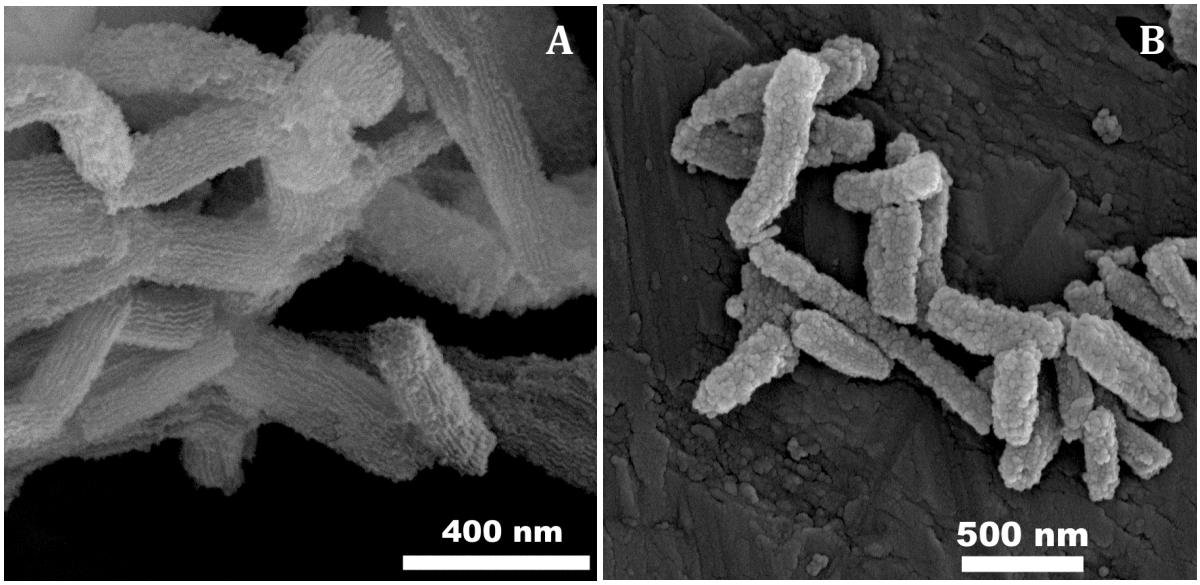

Figure 10. SEM micrographs. **A)** Empty SBA-15 rod-shaped particles. **B)** THY/SBA composite

After loading the EOC into SBA-15, nanoparticles zeta potential was analyzed. Table 5 reports the measurement results. Zeta potential of SBA-15 indicated that it had a good aqueous dispersion stability, in close agreement with results obtained by J. Lillie, who reported potentials of -32.6 mV for SBA-15 [3]. The loading of EOC into SBA-15 resulted in a decrease in the module of negative potential, due to the compound deposited on the material surface. The data corroborated the presence of EOC on the support surface.

Table 5. Zeta potential of EOC/SBA samples.

Nanocomposite	Zeta potential (mV)
SBA-15	-38.4 ± 0.3
CIN/SBA	-14.8 ± 0.6
CRV/SBA	-21.8 ± 1.1
TIM/SBA	-22.1 ± 1.0

When loaded nanoparticles were analyzed by Nitrogen adsorption-desorption method, the amount of absorbed nitrogen decreased compared to the empty sample, as can be seen in Figure 11 for thymol loaded nanoparticles.

The typical hysteresis loop of loaded mesoporous materials is not well defined. The overall nitrogen adsorption amounts decrease for all relative pressures, indicating the presence of EOC adsorbed at the SBA-15 network. [36]. That was also reflected in pore size

distribution. The pore volume distribution diagrams associated with loaded nanocomposites under discussion can be seen in Figure C.2.7 (Annex C.2). The figure clearly illustrates the pore volume reduction from empty particles to the loaded composites, which have free volume lower than 0.05 cm^3/g. Figure B.2.3.C for CRV/SBA and Figure B.2.4.C for CIN/SBA loaded materials show the Nitrogen adsorption-desorption plots. The three samples exhibited the same behavior.

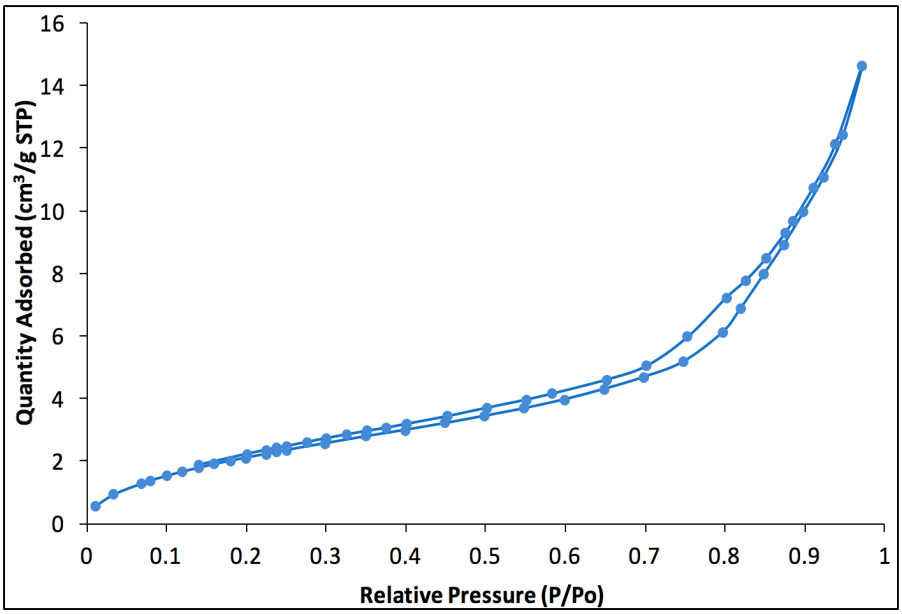

Figure 11. N_2 Adsorption-desorption isotherm of THY/SBA nanocomposite.

The key parameters determined from the N_2 sorption experiments are shown in Table 6. BET surface analysis and pore volume results confirm that EOC molecules fully occupied the original silica mesoporous support void space. In all cases, as expected, BET surface decreased significantly related to empty SBA (around 98%), confirming the loaded material and pore saturation.

Table 6. N_2 adsorption-desorption BET surface area and pore volume.

Nanoparticles	S_{BET} (m^2/g)	Pore Volume (cm^3/g)
SBA-15	661.7	1.5
CIN/SBA	5.0	0.0
CRV/SBA	1.7	0.0
TIM/SBA	7.3	0.0

ATR-FTIR analysis in the region of 600-4000 cm^{-1} was carried out for loaded samples to confirm the presence of EOC on the silica support. Figure 12 shows the FTIR spectra of pure SBA-15, pure thymol and THY/SBA sample.

The SBA-15 spectrum showed the following characteristic bands: 1100 cm^{-1}, 960 cm^{-1} and 800 cm^{-1} that correspond to Si-O-Si, Si-OH and Si-O stretching (st), respectively. Regarding thymol, typical absorption bands according to the spectra were: a strong peak at 800 cm^{-1} for aromatic ring C-H bending, 1280 cm^{-1} owing to isopropyl st, 1240 cm^{-1} for C-O phenolic st. At 1400 cm^{-1} C-C st; peak at 2945 cm^{-1} attributed to C-H methyl group st, and the broadband due to O-H hydroxyl group at 3250 cm^{-1} [39].

The presence of thymol and silica mesoporous support in the nanocomposite were shown mainly by the broad peak at 1100 cm^{-1} from SBA-15, an intense band at 800 cm^{-1}, a doublet at 1400 cm^{-1}, and the methyl group at 2945 cm^{-1} (Figure 12).

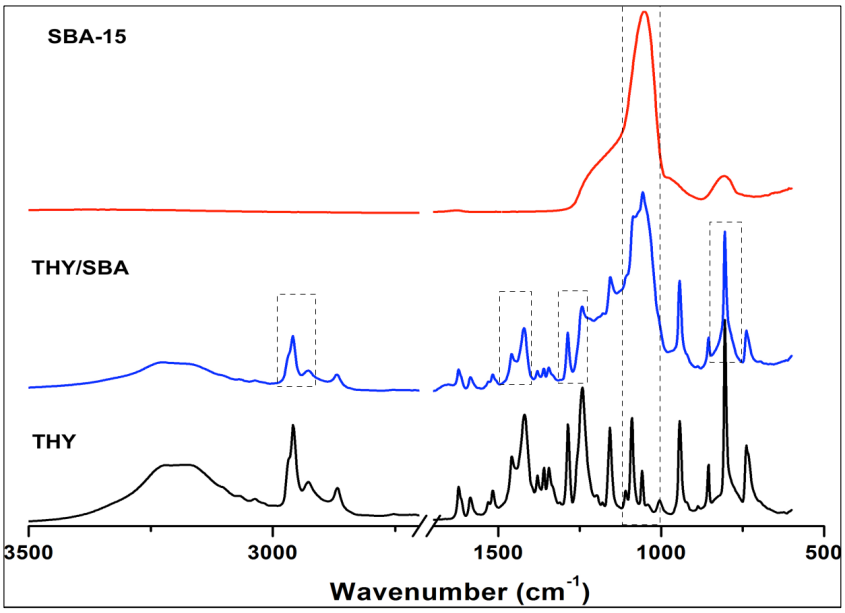

Figure 12. FTIR comparative spectrum for SBA-15, thymol and THY/SBA loaded samples, in absorbance mode

Figure C.2.3.D (Annex C.2) illustrates the FTIR spectrum of CRV/SBA sample. Since the CRV molecule has similar chemical structure and functional groups than thymol, characteristic peaks are related. The spectrum shows peaks at 800 cm^{-1} related to the aromatic ring, in the region from 1340-1460 cm^{-1} for C-H deformation, and at 2960 cm^{-1} and 3300 cm^{-1} regarding C-H st and a hydroxyl group, respectively [40]. Loaded material CRV/SBA combined the characteristic peaks signals from both materials.

FTIR spectrum of CIN/SBA nanocomposite is shown in Figure C.2.4.D. From cinnamaldehyde spectrum, it can be observed an intense C=O band at 1645 cm^{-1} that belongs to the aldehyde group; 1460 cm^{-1} and 1627 cm^{-1} for C=C bond; a signal for aromatic C-H is shown at 3000 cm^{-1}, and the one at 1160 cm^{-1} corresponds to the aromatic C-H signal. [41]. These peaks were presented on CIN/SBA sample, which confirms the cinnamaldehyde presence.

Figure 13 represents the small angle XRD patterns of EOC nanocomposites. The three samples showed the characteristic peaks of SBA-15 at reflections (100), (110) and (200). The presence of EOC loaded into SBA-15 particles and on the material surface, did not result in structural ordering changes. In all cases, the peaks are slightly shifted towards higher angles compared to the SBA-15 due to the filled pores [27]. Experimentally Pikus *et al.* illustrated the shift of (110) and (200) peaks towards higher angles when the pore size is reduced [37]. Furthermore, peak intensity for reflections (110) and (200) are higher than in the unloaded support, according to Pikus *et al.* these peaks are very sensitive to the change of the pore with, which confirms the filled pores of SBA-15 [37].

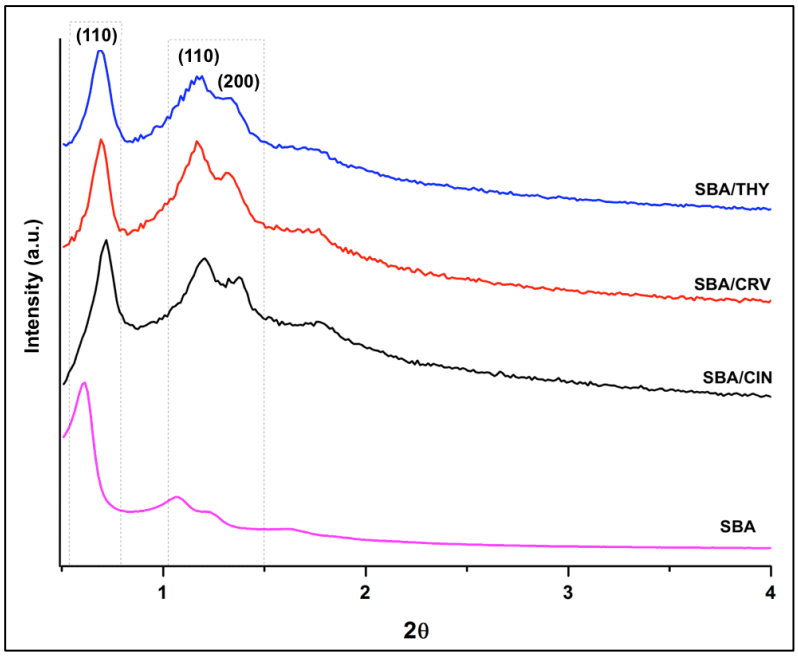

Figure 13. Small Angle X-Ray diffraction pattern for EOC/SBA loaded samples

At this point, information attained from experiments carried out demonstrates that the SBA-15 nanoparticles were successfully filled with essential oil components, leading to the potential use of these particles as EOC carriers.

EOCs release profile

The profile obtained from the *in vitro* release studies carried out in simulated biological fluid are illustrated in Figure 14. Results are expressed as a percentage of EOC released to the medium referred to the loaded mass of the compound according to TGA analysis data.

Two main stages can be recognized from these curves. In the first stage, the system delivered up to 68% for CRV/SBA and 64% for THY/SBA before 48 h. From the profile, a linear controlled release stage can be observed during the first 48 h. These results should be underlined due to the nanocomposite prevention of the compound burst release, phenomena that are commonly associated with drug delivery. This fast compound liberation to the media was stated by Doadrio *et al.*, who reported a gentamicin (hydrophilic drug) initial burst release of 60% in 1 h from SBA particles [14]. On the other hand, Qing-Zhou *et al.* obtained a 50% of Ramipril (hydrophobic drug) released from SBA-15 matrix after 5 h [16]. In our materials, the compounds released from the SBA-15 surface and pores were more sustained in time, which could be attributed to the intramolecular interactions between the EOC molecules as well as intermolecular interactions between the EOC molecules and SBA-15 silanol groups.

The second stage started after 48 h and fulfilled the 100% of compound released (CAR and THY). This event may be attributed to the remaining EOC on the SBA-15 surface and the outlast compound into the pores. The molecules inside the pores form intermolecular hydrogen bonds with the silanol groups of the support, and they are released to the media through the diffusion-controlled mechanism. Moreover, it has been reported that the SMP materials improve the solubility of hydrophobic compounds, enhancing the molecules bioavailability to be released to the medium [42].

Cinnamaldehyde released from the nanocomposite only reached a 24%, but this result is misleading due to the previously mentioned compound decomposition. The quantification of CIN concentration in samples obtained from the release assays was carried out by UPLC. After checking the results, it was considered that they were not feasible due to the compound instability explained above.

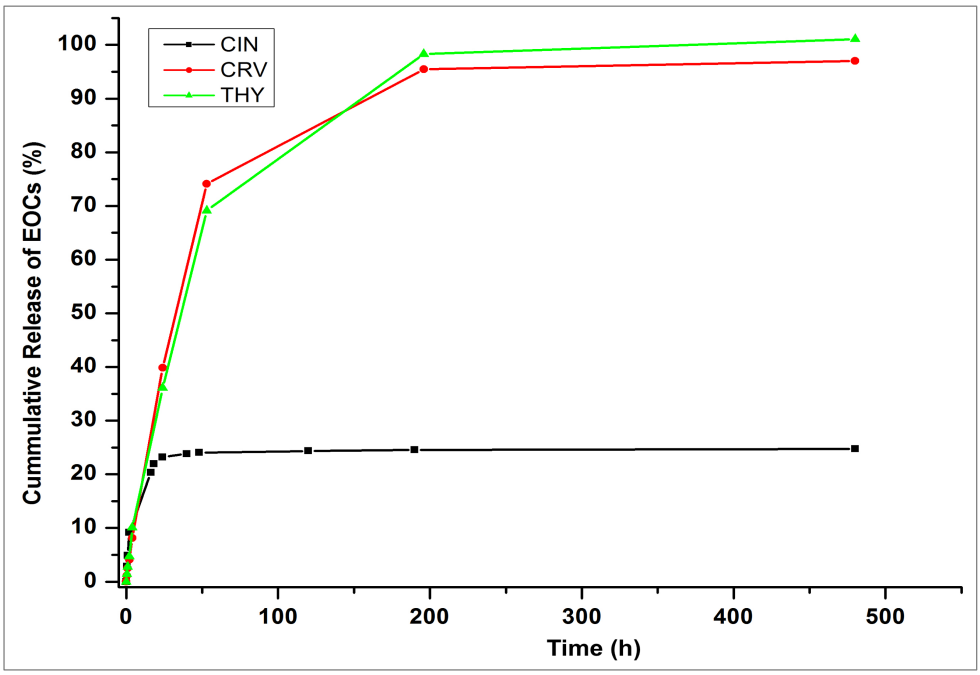

Figure 14. EOCs release profile of loaded samples in body fluid simulator (PBS)

This study is mainly focused on the material performance during the first 48 h, time period in which wound dressings are usually applied (final material application). Our results demonstrated the nanocomposite system functionality to achieve a sustained antimicrobial compound release during the first two days, which ensures the maximum availability of EOC in wound contact.

– **Bactericidal effect of SBA-15 loaded particles**

In vitro antibacterial activity of nanocomposites on *S. aureus* was analyzed by the agar dilution method, in which bacteria cultures were in contact with EOC/SBA-15 nanoparticles for 24 h. Two active compound concentrations were evaluated, the higher was related to the MBC values acquired above from the first objective: CRV 0.3 mg/mL, THY 0.3 mg/mL and CIN 0.5 mg/mL. The second one was a lower concentration to verify their antibacterial activity.

As given in Table 7, empty SBA-15 positive control as expected, did not exert an antimicrobial effect, obtaining similar bacteria concentration as in the control sample in TSB ($2.0x10^9$ CFU/mL).

When SBA-15 nanoparticles loaded with EOC at the free bactericidal concentration (MBC) were tested, all samples exhibited complete inhibition of bacteria growth. It is noteworthy that according to their release profile, during the first 24 h the system

concentration was approximately 0.12 mg/mL for carvacrol nanocomposite, while for thymol composite it was 0.11 mg/mL. These results imply that when the compound is loaded into SBA-15 supports, the minimum concentration required to inhibit the microorganism growth is three times lower than the free compound. The same behavior was displayed by CIN/SBA material, showing a free EOC concentration of 0.11 mg/mL. This is an interesting result, owing to the cinnamaldehyde release profile previously discussed. This result confirms that the CIN and the decomposition products are released from the support, and the measurements from UPLC were not representative because the method only determines *trans*-cinnamaldehyde. Benzaldehyde and *cis*-cinnamaldehyde would be as bactericidal as *trans*-cinnamaldehyde.

The use of lower loaded EOC concentration yielded a decrease in antimicrobial activity. After 24 h, the EOC released amount was nearly 0.07 mg/mL, at least 3 times lower than the MIC value (0.2 mg/mL for CRV and THY, 0.4 mg/mL for CIN) for the free compound, as reported in Table 7. However, a 5 $\log_{10}$ reduction in bacteria concentration was obtained, demonstrating the high antimicrobial activity of loaded nanosystems.

Table 7. Bactericidal activity of loaded nanocomposites on *S. aureus* after 24 h of incubation.

Composite	EOC concentration (mg/mL)*	EOC released after 24 h (mg/mL)**	Bacteria concentration (CFU/mL)
CRV/SBA	**0.2**	0.08	$1.2x10^4$
	0.3	0.12	No growth
THY/SBA	**0.2**	0.07	$1.1x10^4$
	0.3	0.11	No growth
CIN/SBA	**0.3**	0.07	$2.9x10^6$
	0.5	0.11	No growth
SBA	Positive control	$4.2x10^9$ CFU/mL	

* Referred to loaded mass

** Based on the release profile

Based on *in vitro* bactericidal assays, new values of MIC and MBC for carvacrol, thymol, and cinnamaldehyde can be established when are loaded into SBA-15, Table 8 summarizes these results.

Table 8. MIC and MBC values for EOC when are loaded onto SBA-15, compared with the free compound results.

EOC	Free (mg/mL)		Loaded (mg/mL)	
	MIC	MBC	MIC	MBC
Carvacrol	0.2	0.3	0.08	0.1
Cinnamaldehyde	0.4	0.5	0.07	0.1
Thymol	0.2	0.3	0.07	0.1

As previously mentioned, the mesoporous silica materials can improve the solubility of hydrophobic compounds. Thus, the loaded system retains good dispersity in the culture media, resulting in an antimicrobial activity enhancement. Lillie evaluated the bactericidal properties of mesoporous materials loaded with EOC mixtures (cinnamaldehyde-clover) showing 71% of EOC loaded. The system displayed an antimicrobial activity at higher concentrations than 12.5 mg/mL on *S. aureus,* determined by optical density changes [3]. The differences between their results and ours could be attributed to the bactericidal determination method, it lower loading on SMP, and the EOCs employed by the author.

Additionally, it has been reported an antimicrobial capacity enhancement of EOCs when they are encapsulated within different nanocarriers, as a result of an increment of physical stability, prevent from volatility, protection against the environment and enzymatic degradation and ensuring the optimal pharmacokinetic profile [9]. Examples of EOCs nanocarriers developed are: oregano EO loaded into chitosan nanoparticles, thymol encapsulated into zein nanocapsules, and carvacrol into polylactic glycolic acid nanoparticles [9]. Regarding our results, we can confirm that the loading of EOC in silica mesoporous materials as nanocarriers also enhanced their antimicrobial activity.

Besides, it has been reported that microorganisms have a strong tendency to adhere to the inert biomaterial surface and form biofilm through surface fixation and subsequent exopolymer production [43]. Kinnari *et al*. evaluated the *S. aureus* adherence on the SBA-15 surface. They confirmed that in the presence of silica mesoporous support biofilm was formed [43]. Therefore, bacteria tend to be attached to the SBA-15 surface getting in close contact with EOCs enhancing the antimicrobial activity.

These results pointed to an enhanced bactericidal effect against *S. aureus* of thymol, carvacrol, and cinnamaldehyde when they were loaded into SBA-15. Furthermore, the silica framework protected the oil during the handling and storage facilitating and extending the

bactericidal performance, and supporting a sustained compound release for more than 200 h, a period long enough for the wound dressing application [44].

– **Development of PCL fibers attached to SBA-15 rod-shaped nanoparticles**

In our approach to elaborate the mixed SBA/PCL fibers, a technique with two parallel nozzles and a collector drum was used (Figure A.2.1 in Annex A). This configuration promoted the silica nanoparticles deposition on the fiber surface. In one needle, a polymer solution of PCL 10% was used at a flux rate of 1 mL/h. In the second needle, a solution of dispersed SBA-15 rods was utilized, with different flux rate and solution concentration.

In the first procedure, 5 mg/mL of suspended SBA-15 was employed at a flux rate of 1 mL/h. Figure 15 shows electrospun PCL fibers randomly oriented. However, it was clear that a small population of SBA-15 nanorods was deposited on the surface of the fibers.

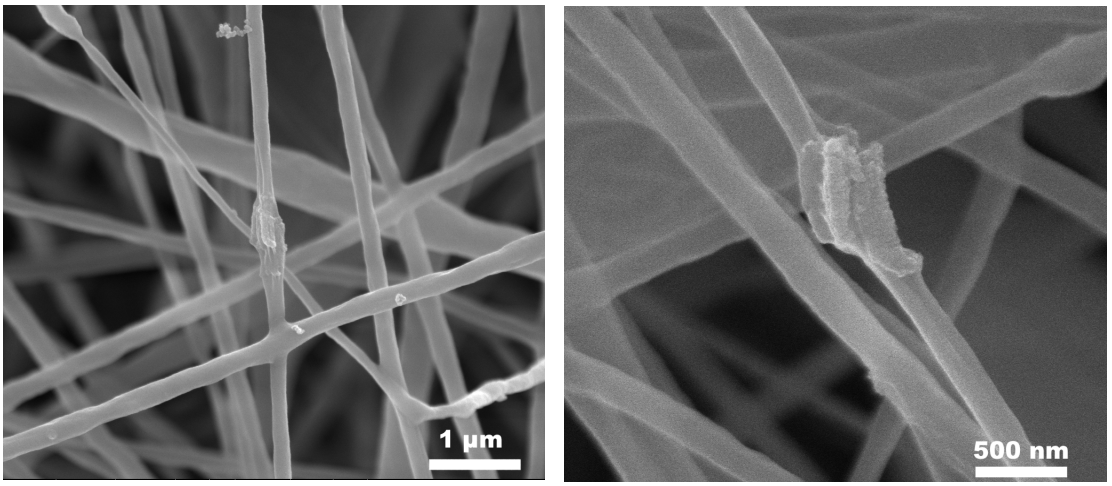

Figure 15. SEM images of fibers loaded with SBA-15 rod-shaped 5 mg/mL at 1mL/h

Aiming to increase the fibers surface available rods, a higher concentration of SBA-15 (15 mg/mL) was employed as well as two suspension flux rates (1 mL/h and 2 mL/h). Figure 16 shows representative micrographs of mixed PCL/SBA-15 composite. There are depicted sphere-shaped SBA-15 aggregates among the PCL fibers with a higher density of the porous material when a higher concentration was utilized. Figure 16.B shows the electrospun material prepared, at an SBA-15 suspension flow rate of 2 mL/h obtaining, as expected, higher silica mesoporous material density by using higher flow rate. Among the flux tested, 2 mL/h was found to be most appropriate. We also corroborated that the two needles technique yielded a well-formed and distributed PCL/SBA-15 hybrid fibers.

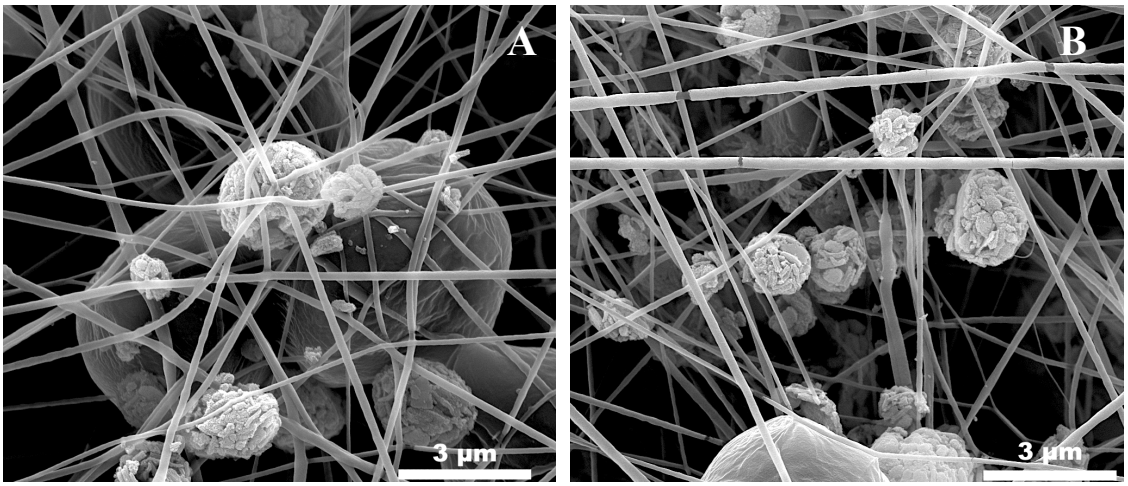

Figure 16. SEM images for SBA-15 nanoparticles deposited on electrospun PCL fibers, using a SBA-15 dispersion of 15 mg/mL. **A)** 1 mL/h. **B)** 2 mL/h.

Intending to avoid the SBA-15 particle aggregation during the electrospinning process, the influence of a previous sonication step of the SBA-15 suspension and the reduction of solid concentration was tested. Figure 17 depicts that this process enables a more homogeneous particle dispersion on the fibers.

When a sonicated suspension of 10 mg/mL of thymol loaded SBA-15 nanoparticles was electrospun at a flow rate of 2 mL/h, it resulted in a successful attachment of THY/SBA particles over the fiber surface. Figure 17 illustrates the representative SEM images of the obtained composite with loaded rods well-dispersed over the fibers.

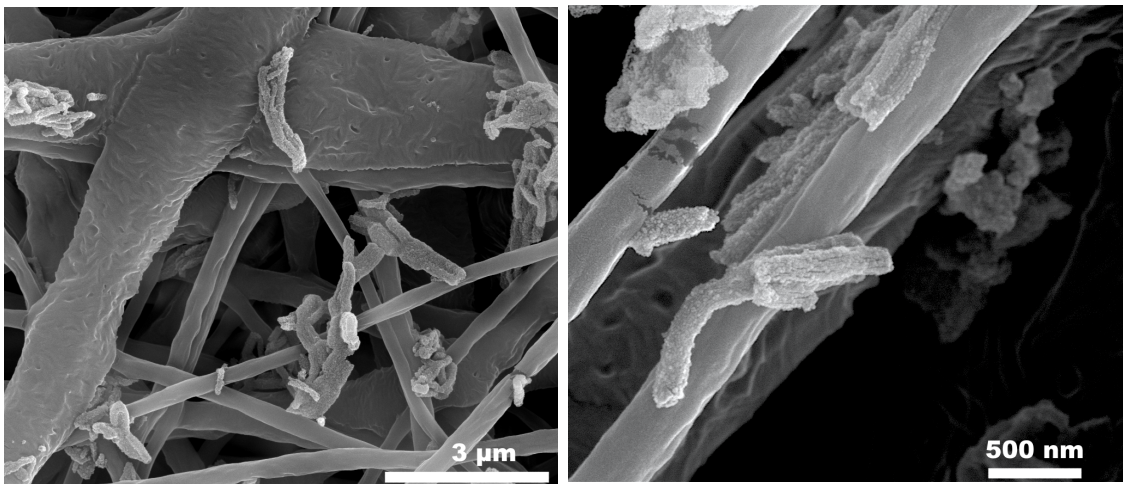

Figure 17. SEM images of electrospun PCL fibers assembled with SBA-15 thymol loaded particles.

However, it remains to be elucidated whether more concentrated EOC/SBA-15 solution and a higher composite suspension flow rate may be used to achieve a higher EOC in the bactericidal hybrid system.

Finally, it can be concluded that the hybrid system has a promising role as wound dressing matrix due to the incorporation of mesoporous materials with a higher EOCs loading, a marked performance in compound release delivery and promising antimicrobial properties for their clinical application.

Future work

Since SBA-15 decorated PCL fibers have been developed in this work to be used as an antibacterial wound dressing, the *in vitro* evaluation of the bactericidal behavior of the PCL/SBA-15 composite loaded with EOCs is necessary for further clinical applications. Furthermore, the *in vitro* evaluation of nanocomposites against a Methicillin Resistant *Staphylococcus aureus* strain is relevant to verify their bactericidal effect to this pathogenic strain.

Besides, the development of a quantitative method to determine the EOC compound content in the prepared composites is important. A possible method is the PCL fibers dissolution with dichloromethane, followed by an EOC extraction, separation of suspended SBA-15 particles and quantification by GC-MS.

The synthesis of hybrid fibers with higher content of EOCs towards the increment of the available amount of antimicrobial compounds to be released could be considered, depending on the bactericidal results regarding the potential application of these smart dressings.

CONCLUSIONS

The specific conclusions achieved during the project include:

- Carvacrol, thymol, and cinnamaldehyde exhibited higher antibacterial activity among tested EOCs showing the lowest MIC and MBC values.
- The loading of THY, CRV and CIN into synthesized SBA-15 was successfully achieved, by the incipient wetness impregnation method, with a highly-concentrated compound solution (5x theoretical pore volume) under 1 h of impregnation time. The use of this concentrate solution promoted the deposition of compound molecules on mesoporous materials, allowing higher antimicrobial load, achieving %LE of 205%, 256% and 267% for CIN, CRV and THY, respectively.
- The analysis performed by N_2 adsorption-desorption of loaded samples confirmed the support pore saturation, with a decrease of BET surface from 661.7 m^2/g to 5.0, 1.7 and

1.6 m^2/g for CIN, CRV and THY, correspondingly. Pore saturation was also confirmed for the pore volume decrement from 1.5 cm^3/g to 0 cm^3/g in all samples.

- The SBA-15 structure was not affected by the loading process, which was corroborated by the XRD patterns showing the typical (100), (110) and (200) peaks with small shifts. ATR-FTIR analysis exhibited the characteristic signals for material support and EOCs. SEM images confirmed the presence of essential oil compounds deposited on the SBA-15 surface.
- The use of SBA-15 as EOC carrier showed a good controlled and sustainably deliver performance, avoiding the burst release. The achieved compounds release was 68% for CRV and 64% for THY during the first 48 h, time in which wound dressings are employed. CIN released results was not accurate due to the analytical problems.
- The loading of EOC into SMP supports enhanced their antimicrobial activity on *S. aureus* in comparison to the free compound. In this regard, lower EOC concentration was required to inhibit the bacteria growth, for CRV and THY decreased from 0.2 mg/mL to 0.1 mg/mL and CIN concentration changed from 0.4 mg/mL to 0.1 mg/mL.
- PCL fibers were successfully joined with thymol loaded SBA-15 nanoparticles, with high-density and well-distributed rods along the fibers.

Summing up, nanostructured SBA-15 was successfully loaded with essential oil compounds (carvacrol/thymol/cinnamaldehyde) with antimicrobial properties and controlled release. The synthesized nanocomposites demonstrated that the antibacterial behavior of these EOCs was enhanced through their entrapment into mesoporous silica supports. Moreover, the loaded system was suitable to be attached to biocompatible fibers, to obtain a hybrid material with the potential application as smart dressings with bactericidal properties.

BIBLIOGRAPHY

[1] Moet *et al*. *Diagnostic Microbiology and Infectious Disease,* vol. 57, pp. 7-13, 2007.

[2] Orchard *et al. Evidence-Based Complementary and Alternative Medicine,* pp.1-92, 2017.

[3] J. Lillie. Doctoral thesis, 2016.

[4] Fife *et al. Wounds,* vol. 24, pp. 10-17, 2012.

[5] Anjuma *et al. International Journal of Pharmaceutics,* vol. 508, pp. 92-101, 2016.

[6] Rieger *et al. Journal of Materials Chemistry B,* p. 4531–4541, 2013.

[7] Andreu *et al. Materials,* vol. 8, pp. 5154-5193, 2015

[8] Ulubayram *et al. Current Pharmaceutical Design,* vol. 21, pp. 1930-1943, 2015.

[9] Rai *et al. International Journal of Pharmaceutics,* vol. 519, pp. 67-78, 2017.

[10] Van Speybroeck *et al. Journal of Pharmaceutical Sciences,* vol.98, pp.2468-2658, 2009.

[11] Pérez-Esteve *et al. Nanotechnology in Nutraceuticals*, 2017, pp. 397-432.

[12] Chaudhary *et al. J Porous Mater,* vol. 24, pp. 741-749, 2017.

[13] Hoffman *et al. Angew. Chem. Int. Ed,* vol. 45, pp. 3216-3251, 2006.

[14] Doadrio *et al. Journal of Controlled Release,* vol. 97, pp. 125-132, 2004.

[15] Sayari *et al. Journal of American Chemical Society,* vol. 126, pp. 14348-14349, 2004.

[16] Qing-Zhou *et al. J Incl Phenom Macrocycl Chem,* pp. 113-120, 2013.

[17] Wang *et al. Materials Chemistry and Physics,* vol. 115, p. 649–655, 2009.

[18] Iwamoto *et al. Pediatrics,* vol. 132, pp. 817-824, 2013.

[19] Klevens *et al. American Medical Association,* vol. 298, pp. 1763-1771, 2007.

[20] P. Lambert. *Journal of Applied Microbiology,* vol. 92, pp. 46S-54S, 2002.

[21] Di Pasqua *et al. J. Agric. Food Chem.,* vol. 55, pp. 4863-4870, 2007.

[22] Shao *et al. Comprehensive Biotechnology*, 2nd Edition ed., vol. 4, 2011, p. 645–658.

[23] Kalemba *et al. Current Medicinal Chemistry ,* vol. 10, pp. 813-829, 2003.

[24] Seow *et al. Food Science and Nutrition,* vol. 54, p. 625–644, 2014.

[25] Bernardos *et al. J Sci Food Agric,* vol. 95, pp. 2824-2831, 2015.

[26] Mellaerts *et al. Langmuir,* vol. 24, pp. 8651-8659, 2008.

[27] D. Carmona, Doctoral Thesis. 2012.

[28] Johanson *et al. Langmuir,* vol. 27, p. 4994–4999, 2011.

[29] Moreira *et al. LWT-Food Science and Technology,* vol. 38, p. 565–570, 2005.

[30] Chlebicki *et al. Am J Infect Control,* vol. 41, p. 167–173, 2013.

[31] Lang-Hong *et al. American Chemical Society,* vol. 64, p. 6355−6363, 2016.

[32] S. Burt. *International Journal of Food Microbiology,* vol. 94, p. 223– 253, 2004.

[33] Shang-Tzen *et al. Journal of Ethnopharmacology,* nº 77, pp. 123-127, 2001.

[34] Ananda *et al. Journal of Dairy Science,* vol. 92, pp. 1423-1429, 2009.

[35] Zengin *et al. Molecules,* vol. 19, pp. 17773-17798, 2014.

[36] Nieto *et al. Langmuir,* vol. 26, pp. 5038-5049, 2010.

[37] Pikus *et al. Applied Surface Science,* vol. 253, p. 5682–5687, 2007.

[38] Friedman *et al. J. Agric. Food Chem.,* vol. 48, pp. 5702-5709, 2000.

[39] Tawakkal *et al. Journal of Applied Polymer Science,* p. 42160, 2016.

[40] Keawchaoon *et al. Colloids and Surfaces B: Biointerfaces,* vol. 84, p. 163–171, 2011.

[41] Al-Bayati *et al. Pharmaceutical Biology,* vol. 47, pp. 61-66, 2009.

[42] S. Wang. *Microporous and Mesoporous Materials,* vol. 117, pp. 1-9, 2009.

[43] Kinnari *et al. Journal of Biomedical Materials Research,* vol. 89A, pp. 215-223, 2009.

[44] Carmona *et al. Microporous and Mesoporous Materials,* vol. 161, p. 84–90, 2012

ANNEX